A Case Study of the Role of Structural/Optical Model Fidelity in Performance prediction of Complex Opto-Mechanical Instruments

Sanjay S. Joshi
joshi@csi.jpl.nasa.gov
(818) 354-0541

James W. **Melody**
jmelody@csi.jpl.nasa.gov
(818) 354-0615

Gregory **W.** Neat
neat@hucy.jpl.nasa.gov
(818) 354-0584

Jet Propulsion Laboratory,
California Institute of Technology
4800 Oak Grove Drive
Pasadena, CA 91 109

Abstract

This paper determines model performance prediction accuracy as a function of model fidelity for a complex opto-mechanical system. The test article is the Micro-Precision Interferometer testbed; a ground-based hardware model of a future spaceborne interferometer. The primary modeling tool is the Integrated Modeling of Optical Systems (IMOS) package. Three models of the MPI testbed were created for this study; each with a unique optical and structural model fidelity. The paper compares disturbance transfer function predictions from the three models with measured disturbance transfer functions from the hardware testbed. Results suggest meaningful model prediction errors exist when simple models are used to represent a complex opto-mechanical system. However, modest increases in model fidelity can lead to significant improvement.

1. Introduction

Discovery of earth-like planets around other stars requires an instrument with micro-arcsecond astrometric measurement accuracy [1, 2]. Spaceborne optical interferometers are likely to be the first instrument class capable of achieving this accuracy level. Although this partial-aperture approach offers a number of important advantages over the traditional full-aperture approach (e.g., the Hubble Space Telescope) the instrument requires stabilization of optical elements down to the nanometer level as well as laser metrology resolution at the picometer level [3]. The charter for the JPL Interferometer Technology Program (1'1'1') is to mitigate risk for this optical interferometer mission class [4]. A number of ongoing complementary activities address these technology challenges. These activities are: integrated modeling methodology development and validation, metrology and vibration hardware testbed development, and flight qualification of the interferometer components. Though all of these activities are necessary to buy down mission risk, it is integrated modeling that ultimately will be used in the mission and instrument design.

Spaceborne optical interferometer models must represent in some form the structure, the optical elements, the control systems (actuator and sensor dynamics), and the disturbance sources. Detailed models of each of these elements for a complex opto-mechanical system is an extremely time consuming and costly task. Furthermore, the larger the model, the more unwieldy it becomes to exercise. Conversely, lower fidelity models may take considerably less time to build and execute. However, the results may be in question if the simple model does not accurately represent the real problem. Careful consideration must be taken to maintain model fidelity where it significantly impacts performance prediction and simplify where it does not.

This paper quantifies the relationship between model prediction accuracy and model fidelity for a specific complex opto-mechanical system. The test article is the Micro-Precision Interferometer (MPI) test bed; a dynamally and dimensionally representative hardware model of a future spaceborne optical interferometer (see Figure 1) [1]. The modeling tool is the Integrated Modeling of Optical Systems (IMOS) package [5, 6]. The integrated modeling methodology combines structural modeling and optical modeling within a common software environment.

Three models of the MPI testbed were created for this study; each with a unique optical and structural model fidelity. Disturbance transfer functions, measured from the attachment point of the primary disturbance source (spacecraft reaction wheel assemblies) to output optical sensors, are the primary measurements used for instrument performance assessment. These transfer functions accurately depict (in a linear sense) the effectiveness of vibration attenuation strategies at achieving nanometer stabilization of optical elements on a large, lightly-damped, flexible structure excited by mechanical vibrations. This paper describes the three models and compares the predicted disturbance transfer functions from each with the

A Case Study of the Role of Structural/Optical Fidelit y in Modeling Complex Opto-Mechanical Instruments

Sanjay ,S. Joshi
joshi@csi.jpl.nasa.gov
(818) 354-0541

James W. Melody
jmelody@csi.jpl.nasa.gov
(818) 354 0615

Gregory w. Neat
neat@huey.jpl.nasa.gov
(818)354 0584

Jet Propulsion Laboratory,
California Institute of Technology
4800 Oak Grove Drive
Pasadena, CA 91109

Abstract

This paper determines model performance prediction accuracy as a function of model fidelity for a complex opto-mechanical system. The test article is the Micro-Precision Interferometer testbed; a .groutlcl-based hardware model of a future spaceborne interferometer. The modeling tool is the Integrated Modeling of Optical Systems (IMOS) package. Three models of the MPI testbed were created for this study; each with a unique optical and structural model fidelity. The paper compares disturbance transfer function predictions from the three models with measured distu - bance transfer functions from the hardware testbed.

1. Introduction

Discovery of cartll-like planets around other stars requires an instrument with micro-arcsecond astromet ric measurement accuracy [1, 2]. Spaceborne optical interferometers are likely to be the first instrument class capable of achieving this accuracy level. Although this partial-aperture approach offers a number of important advan ı- tages over the traditional full-aperture approach (e. g., tile Hubble Space Telescope) the instrument requires stabilization of optical elements down to the nanometer level as well as laser metrology resolution at the picometer level [3]. The charter for the J 1'1, Interferometer Technology Program (1'1'1') is to mitigate risk for this optical interferometer mission class [4]. A number of ongoing complementary activities address these technology challenges. These activities are: integrated modeling methodology development and validation, metrology and vibration hardware testbed development, and flight qualification of the interferometer components. Though all of these activities are necessary to buy down mission risk, it is integrated modeling that ultimately will be used in the mission and instrument design.

Spaceborne optical interferometer models must represent in some form the structure, the optical elements, the control systems (actuator and sensor dynamics), and the disturbance sources. Detailed models of each of these elements for a complex opto-mechanical system is an ext remely t ime consuming and cost ly task. Furthermore, the larger the model, the more unwieldy it becomes to exercise. Conversely, lower fidelity models may take considerably less time to build and execute. 1 lowever, the results may be in quest ion if the simple model does not accurately represent tile real probl em. Careful consideration must be t aken to maint ain model fidelity where it significantly impacts performance prediction and simplify where it does not.

This paper quantifies the relationship between model prediction accuracy and model fidelity for a specific complex opto-mechanical system. The test article is the Micro-Precision Interferometer (MPI) testbed; a dynamically and dimensionally representative hardware model of a future spacel borne optical interferometer (see Figure 1) [1]. The modeling tool is the Integrated Modeling of Optical Systems (IMOS) package [5, 6]. The integrated modeling methodology combines structural modeling and optical modeling within a common software environment.

Three models of the MPI testbed were created for this study; each with a unique optical and structural model fidelity. Disturbance transfer functions, measured from the attach ment point of the primary disturbance source (spacecraft reaction wheel assemblies) to output optical sensors, arc the primary measurements used for instrument performance assessment. These transfer functions accurately depict (in a linear se n se) the effectiveness of vibration attenuation strategies at achieving nanometer stabilization of optical elements on a large, lightly-damp ed, flexible structure excited by mechanical vibrations. This paper describes the three models and compares the predicted disturbance tra nsfer functions from each with the act ual measured disturbance t ransfer funct ion from the testbed.

2. MPI Testbed Description

Figure1 snows a bird's-cyc view of the testbed which contains all the systems necessary to perform a space-

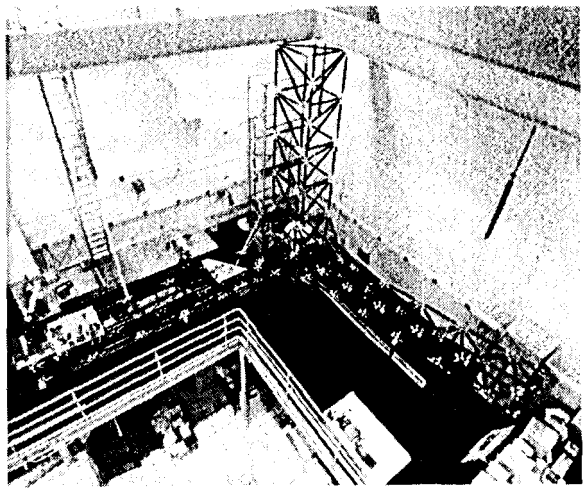

Figure 1: Bird's-eye view of the MPI Testbed.

based, optical interferometer measurement. From the entrance apertures all the way through to the optical detectors, the stellar beam bounces off tweilty-sever] optical surfaces which arc distributed across a 7m truss structure. Three appendages make up the base structure which is composed of drawn-wall aluminum st ruts. The opt ical mounting design strategy was to grou p the optical elements that were close in proximity and mount these groups on independent, locally stiff plates. These plates attached kinematically to the structure. Each individual optic is mounted on a stiff mirror mount which clamps to the respective mounting plate.

The goal for the optical and structural model is to accurately represent the dynamics which couple to the disturbance transfer function with the lowest possible fidelity model. '1'0 determine this desired mode] fidelity, three different MPI structural /optical models were created. A t least two approaches exist to change model fidelity. The first is to place the fidelity in specific components thought to be the major contributors to tile optical metric coupling. For example, place a large amount of fidelity in certain tress struts thought, to couple through local modes to the optical metric while leaving the regions of the truss thought not to couple, as simple beam elements. The second approach is to keep the fidelity constant across similar structural elements. For example, a high fidelity mount model would imply that all mounts are represented by detailed models, not just the mounts thought to couple most closely with the performance metric. Although each method has important implications, this study adopted the latter of these two approaches.

W c describe three models of MPI for this study. In the future, we intend to add more models to span the model fidelity space. The *Low Fidelity* model uses a simple optical model, a simple model for the trusses, mounting hardware and optical mounts. The *Mid-Fidelity* model uses a more complex optical model, a simple truss, more complex mounting hardware and simple optical mount model. The *High-Fidelity* model uses a complex optical model with a complex truss and mounting hardware model.

3. Integrated Model Descriptions

The MPI integrated models consist of a structural finite element model and a linear optical model that are integrated together. Integrated modeling is performed with two software packages: Integrated Modeling of Optical Systems (IMOS) [5] and the Contr olled Optics Modeling Package (COMP) [6]. IMOS is a collection of MATLAB m-files that can be used to perform structural finite element modeling and analysis, optical ray tracing, and thermal analysis. COMP is an optical analysis and modeling program, providing geometric ray-trace, differential ray-trace, and diffraction modeling capability. COMP concentrates on providing detailed opt ical models for integrated design and analysis tasks. In particular, the diffe rential ray-trace capability of COMP can be used to generate linear perturbation models of opt ical systems [6]. The structural model is generated with IMOS, whereas both IMOS and COMP are used to create the optical model. The integration and disturbance analysis are performed in MATLAB with tile aid of IMOS functions.

3.1. Structural Model

Figure 2 shows the *structural* model for both the *Low-Fidelity* and *Mid-Fidelity* models. Figure 3 shows the structural model for the *High-Fidelity* model.

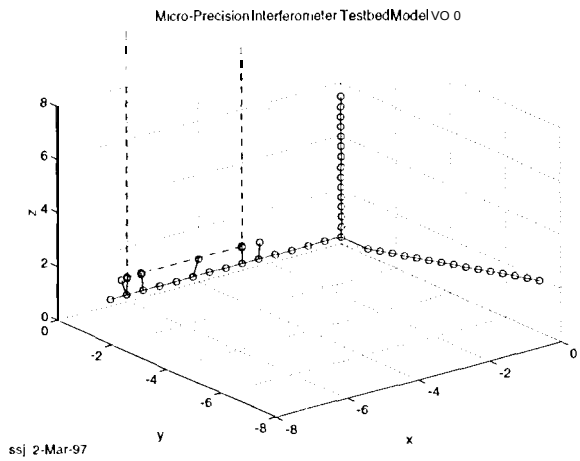

Figure 2: The Low-Fidelity and Mid-Fidelity structural models. Dotted lines show optical path for Low-Fidelity model.

The *Low Fidelity* model consists of three beams to model the MPI truss. Individual strut properties that make up the actual MPI testbed were used to calculate effective beam properties. Optical plates and individual

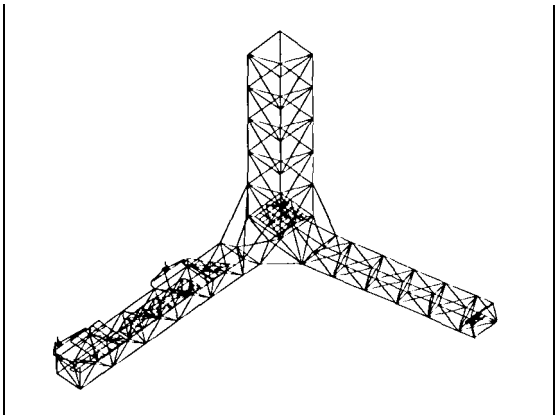

Figure 3: The High-Fidelity model.

component are modeled only as point masses. These include two siderostat masses, two delay line masses, two optical plate masses (which include all optics mounted on them), a metrology beam launcher mass and an isolation system mass. The mounts for the elements are modeled as rigid connections to the beams.

The *Mid-Fidelity* model consists of three beams to represent the MPI truss. individual strut properties that make up the actual MPI testbed were used to calculate effective beam properties. Optical plates and individual component are modeled only as point masses. The mounts for the elements (except the metrology beam launcher mass and isolation system mass) are now modeled as uncoupled, six degree-of-freedom springs from the center of mass of the elements to the beams. The stiffnesses for these springs were derived from high fidelity models of the components.

The *High Fidelity* model consists of plate, beam, truss, and rigid body elements modeling the base truss structure and the attached components (for precise definition of these elements, see [5]). This model has been previously described in [7].

For all models, a modal damping of 0.3% is assumed for the global flexible-body modes, and a damping, where appropriate, of $\approx 3\%$ is assumed for the dynamics associated with the delay line structure. These damping values are consistent with estimates obtained from modal tests.

3.2. Optical Model

The optical model begins with a specification of the optical prescription. This prescription includes the shapes, positions, and orientations of the optical elements. Once the optical prescription is specified, it is exported to COMP where a linear optical model is created. This linear model is calculated by performing an analytic differential ray trace [6]. The optical output can be pathlength, wavefront tilt, or spot motion. For this model fidelity study, the output is pathlength difference.

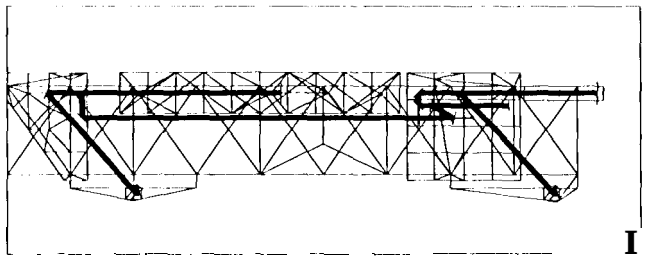

Figure 4: The High-Fidelity optical model.

The *Low Fidelity* optical model (Figure 2) contains five optical surfaces: two siderostats, two beam combiner mirrors, and a fringe detector. The *Mid-Fidelity* optical model (not shown) contains ten optical surfaces: two siderostats, one steering mirror, four delay line mirrors, two beam combiner mirrors, and a fringe detector. Finally, the *High Fidelity* optical model (Figure 4) contains 27 optical surfaces which matches exactly the number in the MPI testbed. More details of the MPI optical train are given in [8].

3.3. Structural-Optical Model Integration

Once the structural and optical models have been created, they are integrated to form a structural-optical model. This integrated model is specified in first-order, state-space form, lending itself most easily to analysis and control synthesis with misting MATLAB functions.

First, the structural model is truncated to remove modes above the bandwidth of expected disturbances (i. e., above 900 Hz) [9]. The truncated modal model is then converted into first-order, state-space form [5, 7]. Finally, the linear optical model is incorporated. The resulting model has disturbance forces as input for example. The output is stellar optical path difference.

Table 1 gives an overview of important features of each of the three models after integration.

Comparison of MPI Models			
-	No. DOF	No. Modes	No. Opt. Elems.
Low	336	92	5
Mid	372	112	10
High	2577	579	27

Table 1: Comparison of number degrees of freedom, number of modes under 900 Hz, and number of optical elements

4. Comparison Method

4.1. Approach

Interferometer performance is primarily degraded by variation in optical pathlength difference (01'1)), i.e., the difference in the distances that the light t ravels from the stellar source, through each arm of the interferometer to the interference optical detector. This difference must be stabilized to the 10 nm (RMS) level in the on-orbit mechanical disturbance environment. It is expected that the dominant disturbance will be the high frequency harmon - ics from the reaction wheel assemblies that result from bearing imperfections, wheel imbalances, etc.

in contrast to estimating modal characteristics as in [10, 11], disturbance input (at the reaction wheel location) to stellar OPD output transfer functions were measured since they completely characterize (in a linear sense) the propagation of disturbances to OPD. Therefore, in this St udy, these disturbance transfer functions wer predicted by the three different models and compared with the measured disturbance transfer function from the testbed.

4.2. MPI Measurement

Figure 5 shows the disturbance input locat ion relative to the *0} '1)* output location for the M 1'1 testbed. This disturbance transfer function was measured for three force disturbance directions: (x, y, z). An 111' data analyzer was used to collect the data. A 10 N shaker, mounted at the base of the tower, applied the force input in each of the three directions. The force input was measured with a load cell mounted between the shaker and the structure. The analyzer calculated the transfer function from force input to OPD output.

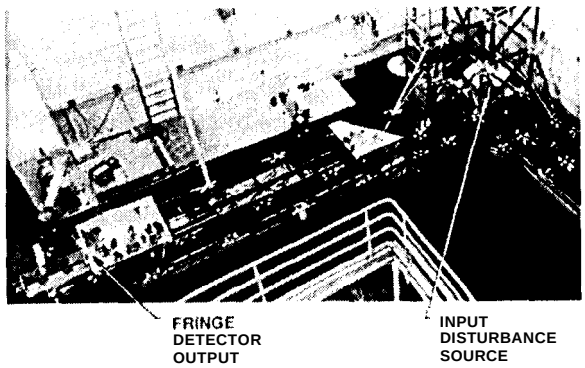

Figure 5: Locations of disturbance input and OPD output on the MPI testbed.

4.3. Comparison Metric

In general on space-based interferometers, mechanical disturbances will be either broadband or narrowband with the energy varying over broad frequency ranges as a function of time [12, 9]. In either case, the power spectral density of the disturbance is broadband. Therefore, the integrated model should be accurate in a broadband sense. More specifically, we desire σ_{opd} to be accurate, where [13]:

$$\sigma_{opd}^2 = \frac{1}{\pi}\int_0^\infty |G(j\omega)|^2 \Phi_d(\omega) d\omega \qquad (1)$$

for a broadband disturbance power spectral density, $\Phi_d(\omega)$, and a disturbance to OPD transfer function, $G(j\omega)$.

Since Equation 1 yields the quantity that we wish to accurately predict, we can use this same equation as a metric to characterize the measured and predicted transfer functions. As opposed to picking a particular expected disturbance power spectral density, bandlimited white noise (over $[\omega_{min}, \omega_{max}]$) is used:

$$\sigma_g^2 = \frac{A_d}{\pi}\int_{\omega_{min}}^{\omega_{max}} |G(j\omega)|^2 d\omega \qquad (2)$$

where A_d is the amplitude of the bandlimited white noise disturbance power spectral density with ω_{min} and ω_{max} defining the frequency range of interest. σ_g is used instead of σ_{opd} in order to stress that the result is a metric of the transfer function itself.

Using this metric, the accuracy of the model can be quantified by comparing σ_g for the *Low Fidelity*, *Mid-Fidelity*, *High Fidelity* and measured transfer functions. As Such) the particular value of the disturbance amplitude is immaterial. The amplitude is chosen so that the variance of the disturbance is one. This choice is arbitrary, and the value of σ_g has no significance by itself. It is the *comparison* oft he metrics for corresponding measured and predicted t ransfer functions t hat is meaningful.

4.4. Results

The modulus of the measured transfer function, along with the corresponding predicted transfer functions, are shown for the z-force input disturbance to OPD output case (Figures 6-8). The predicted transfer functions were calculated by applying standard MATLAB functions to the integrated models with disturbance force input and 0 1'1) output.

The results of comparisons for .2 force inputs are shown in Table 2. The trends are similar for the x and y directions.

The bandwidth of interest is [4, 900] Hz. Below 4 Hz the force capability of the shaker is limited and the testbed suspension modes pollute the measurement. Above 900 Hz the mechanical disturbances are expected to have no energy. This bandwidth is farther broken roughly into decades and comparisons are shown for these "decades." Units are not given in the table so as to discourage the reader from attaching significance to the separate values. All numbers are normalized with respect to the measured values.

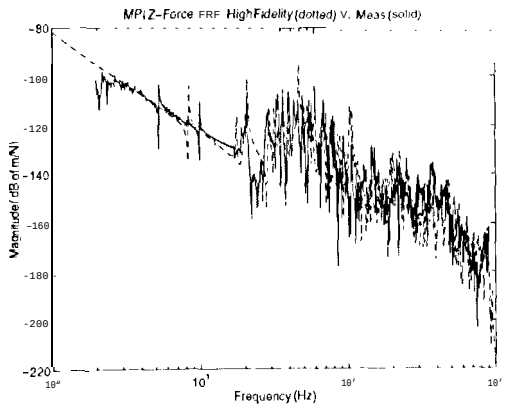

Figure 6: Comparison of measured data from test article to Higll-fidelity model MPI disturbance to OPD transfer function: z-axis form input.

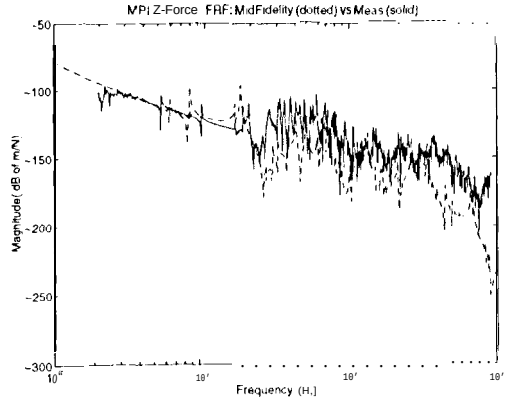

Figure 7: Comparison of measured data from test article to Mid-fidelity model M 1'1 dist urbance to OPD transfer function: z-axis force input.

5. Conclusion/Future Work

This paper investigates the model prediction capabilities of models of varying' structural and optical complexity. A metric is used that characterizes the disturbance transfer functions over a broad frequency range. This metric is simply the expected OPD variation assuming a bandlimited white noise disturbance input. Comparison of the three models shows that a *High-fidelity* model predicts test results well, especially in the 4-100 Hz frequency range. In the high frequency range (100 -900 Hz), the *High-fidelity* model underpredicts. The *Low-fidelity* model snows good performance in the low frequency range (4 - 10 Hz) and a degradation in performance at higher frequencies. This is to be expected since the simple beam model will capture global modes well, but not local modes caused by individual mounts or truss elements. The *Mid-fidelity* model added mount models. This increased performance of the model, especially in the mid frequency range. Analysis of this range shows that most mount modes were located in

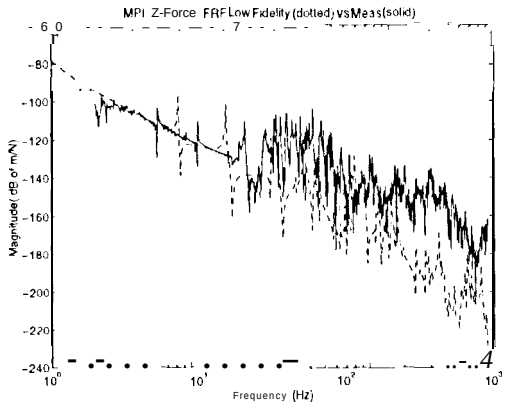

Figure 8: Comparison of measured data from test article to 1,otv-fidelity model MPI disturbance to OPD transfer function: z-axis force input.

Disturbance Input		σ_g			
		4 - 10 Hz	10 - 100 Hz	100 - 900 Hz	4 - 900 Hz
z-axis Force	Low	0.793	0.362	0.246	*0.489*
	Mid	1.212	0.741	0.352	*0.863*
	High	1.013	1.013	0.970	*1.012*
	Test	1.000	1.000	1.000	*1.000*

Table 2: Broadband transfer function metric comparison between the low-fidelity model, mid-fidelity model, high fidelity model and measured transfer functions of the MPI Testbed. All numbers normalized with respect to measured values.

this rail.gc. Overall, the modest increase in fidelity from t he *Low-fidelity* to *Mid-Fidelity* model helped performance greatly. In the future, we intend to add higher fidelity models in our suite of models to judge when adding more fidelity to models leads to a diminishing rate of returns.

References

[1] G. W. Neat, A. Abramovici, J. W. Melody, R. J. Calvet, N. M. Nerheim, and J. F. O'Brien, Wont rol technology readiness for spaceborne optical interferometer missions," in *Proc. Spa cc Microdynamics and Accurate Control Symposium*, (Toulouse, France), May 1997.

[2] B. F. Burke, cd., *TOPS: Towards Other Planetary Systems*. Washington, 1). C.: National Aeronautics and Space Administration, Solar System Exploration Division, 1992.

[3] M. Shao and D. M. Wolff, "Orbiting stellar interferometer," in *Spaceborne Interferometry 1/* (R. 1). Reasenberg, *ccl.*), vol. 2447 of *Proc. SPIE*, (Orlando, FL), pp. 228 239, Apr. 1995.

[4] 1[. A. Laskin, "Technology for space optical interferometry," in *Proc. 33rd Aerospace Sciences Meeting and Exhibit*, vol. 95-0825, (Reno, NV), Al AA, Jan. 1995.

[5] M. 11. Milman, H. C. Briggs, W. Dedeboer, J. W. Melody, R. L. Norton, and L. Needels, *Integrated Modeling of Optical Systems User's Manual, Release* 2.0, Nov. 1995. JPLD 13040 (JPL Internal Document).

[6] D. Redding, *Controlled Optics Modelling Package User Manual, Release 1.0*, June 1992. JPL D 9816 (JPL Internal Document).

[7] J. W. Melody and G. W. Neat, "ltlte-grated modeling methodology validation using the micro-precision interferometer testbed," in *Proc. 35th IEEE Conference on Decision and Control*, vol. 4, (Kobe, Japan), pp. 4222 4227, Dec. 1996.

[s] G. W. Neat, J. F. O'Brien, N. M. Nerheim, R. J. Calvet, H. Singh, and S. Shaklan, "Micro-precision interferometer testbed: First stabilized stellar fringes," in *Spaceborne Interferometry II* (R. D. Reasenberg, ed.), vol. *2447* of *Proc. SPIE*, (Orlando, FL), pp. 104 115, Apr. 1995.

[9] S. Shaklan, J. Yu, and 11. C. Briggs, "Integrated structural and optical modeling of the orbiting stellar interferometer," in *Space* Astronomical *Telescope and Instrument 1/*, Proc. SPIE, (Orlando, FL), Apr. 1993.

[10] M. B. Levine-West and J. W. Melody, "Model updating of evolutionary structures," in *Proc. 15th ASME Biennial Conference on Mechanical Vibration and Noise*, (Boston, MA), Sept. 1995.

[11] J. W. Melody and M. B. Levine-West, "High fidelity modeling of evolutionary structures in IMOS," in *Proc. First World Conference on Structural Control*, (Los Angeles, CA), pp. WP1-98 to WP1-107, Aug. 1994.

[12] J. W. Melody and H. C. Briggs, "Analysis of structural and optical interactions of the precision optical interferometer in space (POINTS)," in *Spaceborne Interferometry* (R. D. Reasenberg, ed.), vol. 19-47 of *Proc. SPIE*, (Orlando, FL), pp. 44 57, Apr. 1993.

[13] A. Papoulis, *Probability, Random Variables, and Stochastic Processes*. New York: McGraw-Hill, 3rd ed., 1()!)].